

## High-quality nanothickness single-crystal $\text{Sc}_2\text{O}_3$ film grown on Si(111)

M. Hong,<sup>a)</sup> A. R. Kortan, P. Chang, Y. L. Huang, C. P. Chen, and H. Y. Chou  
*Department of Materials Science and Engineering, National Tsing Hua University, Hsin Chu, Taiwan*

H. Y. Lee  
*National Synchrotron Radiation Research Center, Hsin Chu, Taiwan*

J. Kwo  
*Department of Physics, National Tsing Hua University, Hsin Chu, Taiwan*

M.-W. Chu and C. H. Chen  
*Center for Condensed Matter Sciences, National Taiwan University, Taipei, Taiwan*

L. V. Goncharova, E. Garfunkel, and T. Gustafsson  
*Departments of Physics and Chemistry, Rutgers University, Piscataway, New Jersey 08854*

(Received 20 May 2005; accepted 22 October 2005; published online 12 December 2005)

High-quality single-crystal  $\text{Sc}_2\text{O}_3$  films a few nanometer thick have been grown epitaxially on Si (111) despite a huge lattice mismatch. The films were electron-beam evaporated from a  $\text{Sc}_2\text{O}_3$  target. Structural and morphological studies were carried out by x-ray diffraction and reflectivity, atomic force microscopy, high-resolution transmission electron microscopy, and medium-energy ion scattering, with the initial epitaxial growth monitored by *in situ* reflection high-energy electron diffraction. The films have the cubic bixbyite phase with a remarkably uniform thickness and high structural perfection. The film surfaces are very smooth and the oxide/Si interfaces are atomically sharp with a low average roughness of 0.06 nm. The films are well aligned with the Si substrate with an orientation relationship of  $\text{Si}(111)\parallel\text{Sc}_2\text{O}_3(111)$ , and an in-plane epitaxy of  $\text{Si}[\bar{1}10]\parallel\text{Sc}_2\text{O}_3[\bar{1}01]$ . © 2005 American Institute of Physics. [DOI: 10.1063/1.2147711]

$\text{Sc}_2\text{O}_3$  has recently gained attention due to its effective passivation on GaN, and its usage as a gate dielectric in GaN-based metal-oxide-semiconductor devices.<sup>1</sup> Unexpectedly,  $\text{Sc}_2\text{O}_3$  thin films were found to grow epitaxially on Si (111) (Refs. 2 and 3) and sapphire<sup>4</sup> with excellent crystal quality.  $\text{Sc}_2\text{O}_3$  is also attractive as an alternative gate dielectric for Si (Ref. 3) due to its relatively high dielectric constant, large band gap, and thermodynamic stability with Si. High-resolution x-ray diffraction studies on single-crystal films 18 nm in thickness, electron-beam (e-beam) evaporated from compacted powder pacts of  $\text{Sc}_2\text{O}_3$  in an ultrahigh vacuum (UHV), have shown a high-intensity and persistent Pendellösung fringe oscillations around the  $\text{Sc}_2\text{O}_3$  (222) diffraction peak and narrow rocking curves of  $\text{Sc}_2\text{O}_3$  (222) and (444).<sup>2</sup> These films were of the bulk bixbyite cubic phase with high structural perfection, sharp interface with Si, and the (111) axis of the oxide films parallel to the substrate normal. The cone scans of the  $\text{Sc}_2\text{O}_3$  {440} and Si {220} diffraction peaks about the surface normal indicated a 60° symmetric rotation of the film with respect to the substrate. High-resolution transmission electron microscopy (HRTEM) studies by Klenov *et al.*<sup>3</sup> on extended defects in a 35 nm thick epitaxial  $\text{Sc}_2\text{O}_3$  film, prepared using reactive molecular-beam epitaxy (MBE) with a Sc flux in an  $\text{O}_2$  background, have shown the formation of a hexagonal misfit dislocation network and a high density of planar defects and threading dislocations.

In this letter, we report the attainment of very high-quality cubic  $\text{Sc}_2\text{O}_3$  single-crystal films with a thickness in the regime from 3 to 4 nm, which is at least six to ten times thinner than what has been published earlier. These nano-

scale films enable us to study the structural quality in the initial stages of growth, and to understand their interface characteristics, based on studies using high-resolution x-ray diffraction in a synchrotron radiation source, x-ray reflectivity, HRTEM, and medium-energy ion scattering (MEIS) (a lower-energy high-resolution variant of Rutherford back-scattering spectroscopy).<sup>5</sup> HRTEM specimens were prepared with mechanical polishing, dimpling, and ion milling using a Gatan PIPS system operated at 3 kV. HRTEM was performed on a field-emission microscopy (Tecnai G<sup>2</sup>) operated at 200 kV.

Small-angle x-ray reflectivity provides valuable information about the film thickness, the interfacial roughness, and the electron density distribution.<sup>6</sup> By using the modeling fits of Bede<sub>REFS</sub> Mercury Code,<sup>7</sup> we were able to determine these parameters. The synchrotron x-ray experiments were performed at wiggler beamline BL17B1 at the National Synchrotron Radiation Research Center, Hsinchu, Taiwan. The incident x rays were focused vertically with a mirror and monochromatized to 10 keV energy by a Si (111) double-crystal monochromator. The sagittal bending of the second crystal focused the x rays in the horizontal direction. The dimensions of beam size are about 2 mm × 0.2 mm ( $H \times V$ ) at the sample position. With two pairs of slits between sample and detector, typical wave-vector resolution in the vertical scattering plane was set at  $\sim 0.01 \text{ nm}^{-1}$ . High-resolution single-crystal x-ray measurements were carried out in the single-crystal geometry.

Substrate Si (111) wafers were placed into a multichamber MBE/UHV system,<sup>8</sup> following Radio Corporation of America cleaning and HF dipping. A Si (111) surface with a streaky (7 × 7) reflection high-energy electron diffraction (RHEED) pattern and Kikuchi lines were obtained following a wafer heating to  $\sim 750^\circ\text{C}$ . The wafers were then trans-

<sup>a)</sup>Electronic mail: mhong@mx.nthu.edu.tw

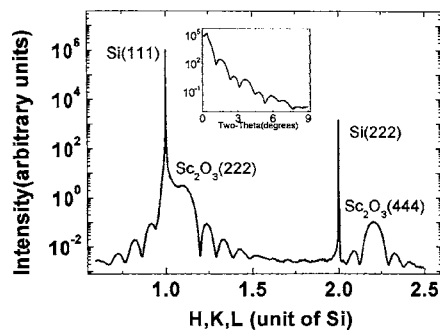


FIG. 1. Single-crystal scans along the surface normal in reciprocal space finds an epitaxial growth of the  $\text{Sc}_2\text{O}_3$  bixbyte phase.

ferred under UHV to an oxide chamber for the  $\text{Sc}_2\text{O}_3$  deposition, in which e-beam evaporation of a pure powder-packed  $\text{Sc}_2\text{O}_3$  source occurred at substrate temperatures in the range of 400–770 °C. During the oxide deposition, the pressure in the chamber was in the low  $10^{-9}$  Torr range. After an  $\sim 0.7$  nm thick oxide was grown, bright streaky ( $4 \times 4$ ) RHEED film patterns were observed along the major in-plane axes of Si ( $[\bar{2}20]$  and  $[\bar{2}02]$ ), indicative of two-dimensional growth and an in-plane alignment between the oxide film and the Si substrate (not shown). After the oxide growth, a 2.4 nm thick amorphous Si cap layer was deposited *in situ* on  $\text{Sc}_2\text{O}_3$  for protection.

The oxide films grow with their  $[111]$  axis parallel to the  $[111]$  Si substrate normal, and the  $[\bar{4}04]$  in-plane axis parallel with the substrate  $[\bar{2}20]$  direction. The rocking scans at  $\text{Sc}_2\text{O}_3(222)$  position of the 3 nm film show a small full width at half maximum (FWHM) of  $0.03^\circ$ , indicative of a high-quality single-crystal oxide film. Atomic force microscopy showed a very smooth surface of a root-mean-square roughness of 0.1–0.2 nm. The oxide/Si interface is also atomically smooth with a value of 0.06 nm as determined by x-ray reflectivity, and is free of  $\text{SiO}_2$  as found by cross-sectional HRTEM and MEIS.

Figure 1 shows single-crystal scan in reciprocal space along the surface normal. The scattered intensity is displayed over nine orders of magnitude of dynamic range, and the horizontal axis displacement is displayed in terms of reciprocal space units of the silicon substrate, i.e., the values of  $H$ ,  $K$ , and  $L$  given in this letter are expressed in reciprocal lattice units (r.l.u.) referred to the Si lattice parameter, 0.357 nm at 295 K. For surface normal scan, reciprocal lattice unit vectors  $\mathbf{H}$ ,  $\mathbf{K}$ , and  $\mathbf{L}$  are set equal to each other, and are all incremented by equal amounts. The broad range covered in Fig. 1 displays substrate peaks (111) and (222), and also (222) and (444) peaks of the bixbyte phase of the  $\text{Sc}_2\text{O}_3$  epitaxial film. Peak positions of the film along the surface normal agree well with the bulk lattice constant of  $\text{Sc}_2\text{O}_3$ , indicating that the epitaxial film is fully relaxed. The well-defined fringe patterns about the Bragg peaks of the film confirm a highly uniform film thickness. The period of the fringe pattern suggests a film thickness of 3.4 nm, in agreement with a value of 3.59 nm determined from x-ray reflectivity (as shown in the inset of Fig. 1).

The rocking scans of the substrate and the films observed in Fig. 1, are shown in Fig. 2. The substrate Si(111) peak exhibits a FWHM value of  $0.005^\circ$ , while the film  $\text{Sc}_2\text{O}_3$  peaks (222) and (444) exhibit FWHM values of  $0.033^\circ$  and  $0.044^\circ$ , respectively. The film peak shapes are not symmetric

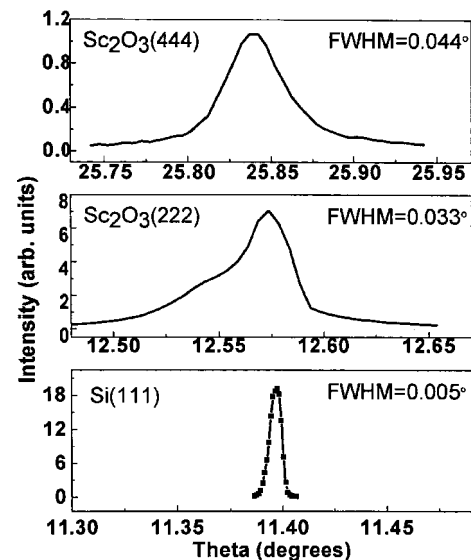


FIG. 2. Rocking (mosaic) scans of the substrate and the epitaxial film peaks.

about the center, as would have been expected from fully strain relaxed film growth. Since relaxation incorporates structural defects like misfit dislocations at the interface (discussed later in the text), the film peaks will broaden in these rocking scans. Considering that the film is fully relaxed, these mosaic spread values are remarkably small. Other samples we measured correlated well with the reported sample. In these fully relaxed films, rocking curve variations are not significant. Characteristic inclined defects can also explain the selective broadening of the (222) peak as shown in Fig. 2. Distinct crystallographic defects, such as antiphase boundaries, do selectively affect some of the Bragg peaks.

The single-crystal scans carried out in other parts of the reciprocal space (not shown) found that, while the  $\langle 111 \rangle$  axes of the silicon substrate and the  $\text{Sc}_2\text{O}_3$  film are well aligned, the two cubic cells are in-plane rotated by  $60^\circ$  with respect to each other. These observations were made on full cone scans about the  $\langle 111 \rangle$  axis that intersect  $\{440\}$  Bragg peaks.

A radial scan ( $-H, K, 0$ ) along the in-plane  $\langle \bar{2}20 \rangle$  direction was measured, with this zone axis lying completely in the surface plane of the substrate, with no out-of-plane component. Along this axis, we find Si  $(\bar{2}20)$  Bragg reflection, as well as the  $\text{Sc}_2\text{O}_3$   $(\bar{4}04)$  peaks, at a fully relaxed lattice constant value.

Figure 3 shows a representative cross-sectional HRTEM image of the  $\text{Sc}_2\text{O}_3/\text{Si}(111)$  heterostructure along  $[11\bar{2}]_{\text{Si}}$  projection. A careful examination of the experimental contrast indicates the epitaxial growth of  $\text{Sc}_2\text{O}_3$  on Si with the orientation relationship of  $(111)_{\text{Sc}_2\text{O}_3} \parallel [1\bar{1}0]_{\text{Sc}_2\text{O}_3} \parallel (111)_{\text{Si}} \parallel [1\bar{1}0]_{\text{Si}}$ . Considering the symmetry elements of  $\text{Sc}_2\text{O}_3$  (Ia-3), the electron diffraction-based HRTEM, viewing in projection, cannot distinguish the in-plane rotation of  $\text{Sc}_2\text{O}_3$  by  $60^\circ$ . Nevertheless, an edge-type misfit dislocation with the line direction parallel to  $[11\bar{2}]_{\text{Si}}$  can be observed (see “T” in Fig. 3). Note that the same type of dislocation was recently reported in 35 nm thick  $\text{Sc}_2\text{O}_3(111)$  films grown on Si(111) exhibiting a regularly spaced ( $\sim 1.8 \pm 0.1$  nm) network,<sup>3</sup> in good agreement with the theoretical spacing of  $\sim 1.9$  nm for a dislocation accommodated mismatch system. Compared to the work on

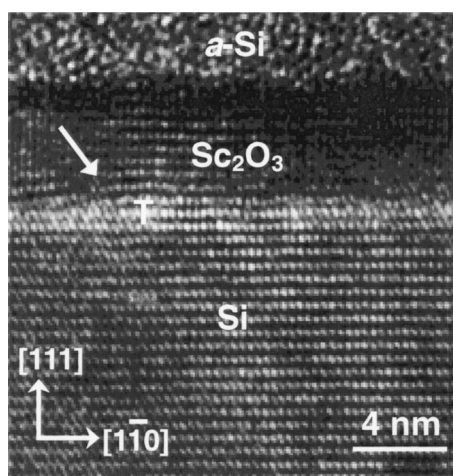


FIG. 3. A cross-sectional HRTEM image of the  $\text{Sc}_2\text{O}_3/\text{Si}(111)$  heterostructure in  $[11\bar{2}]_{\text{Si}}$  projection, showing the  $\text{Sc}_2\text{O}_3$  film thickness of  $\sim 4$  nm. The edge-type misfit dislocation is indicated by "T." The arrow exhibits the inclined defects in  $\text{Sc}_2\text{O}_3$ .

relatively thick films,<sup>3</sup> the absence of a regular dislocation network in Fig. 3 could be a consequence of the film thickness. In ultrathin film heterostructures,<sup>9</sup> the *elastic* accommodation of an in-plane misfit strain is believed to be a complementary strain relief mechanism to the dislocation network formation. Moreover, the kinetics of the elastic accommodation can be complicated by the dynamic film growth conditions and the early nucleation characteristics,<sup>9</sup> potentially leading to the absence of a dislocation network in our ultrathin films. However, the residual strain in the ultrathin  $\text{Sc}_2\text{O}_3/\text{Si}(111)$  may be further relaxed by the inclined defects in  $\text{Sc}_2\text{O}_3$  (see the arrow in Fig. 3). The particularly bright contrast at the interface (see Fig. 3) could be also relevant to the strain effect, and a detailed study is under way.

The density of the inclined defects in our sample was estimated to be  $\sim 10^{14} \text{ m}^{-2}$ . This value is considerably low compared to that of the line defect, misfit dislocations ( $>10^{16} \text{ m}^{-2}$ ), frequently observed in epitaxial heterostructures. Since neither considerable inclined defects nor extensive dislocation networks were observed in the current system, we would expect that the corresponding rocking scans are little affected by such crystallographic defects.

Figure 4 shows a MEIS backscattering energy spectrum for an uncapped  $\text{Sc}_2\text{O}_3$  film exposed to air prior to analysis. The measurement was done in a double-alignment geometry in the Si  $[\bar{1}\bar{1}2]$  scattering plane, with the incoming beam aligned with a  $[111]$  channeling direction and the detector axis aligned with a Si  $[001]$  axis. Observation of distinct blocking minima in a Sc signal, shown in the inset in Fig. 4, and a comparison of the Sc signal just below the surface Sc peak to a calculated yield for the same thickness amorphous film (the yield, shown as a dashed line in Fig. 4) indicate very good film crystalline quality. Surface carbon species were detected ( $\sim 2 \times 10^{15} \text{ atoms/cm}^2$ ) due to the air exposure. Remarkably, no interfacial Sc and O peaks are observed, indicating a highly ordered  $\text{Sc}_2\text{O}_3$  lattice structure at the interface with Si. The small additional visibility of Si atoms at the interface (compared to an ideal bulk-terminated lattice) suggests good crystallinity of the interface with possibly some quite minor deformation or defect formation of the Si lattice.

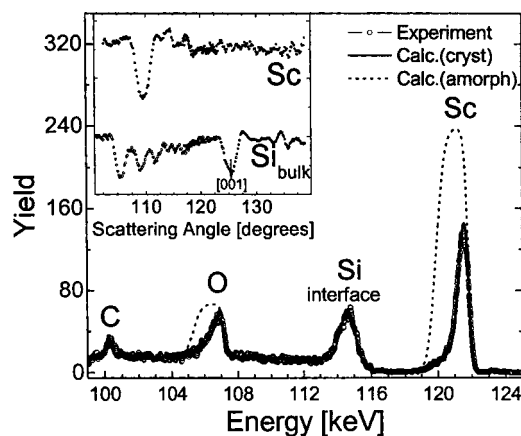


FIG. 4. Backscattering energy spectrum ( $130 \text{ keV H}^+$ ) of a  $\text{Sc}_2\text{O}_3$  film on Si(111) in a normal incidence and substrate blocking geometry. A simulation (solid line) shows a fit for a 3.9 nm thick crystalline film with no detectable interfacial layer formation, to be compared to a simulation for an amorphous film (dashed line). The inset shows angular distributions for the Si and Sc signals.

The angular distribution of the Sc yield shows no evident minima when the detector is aligned with the Si substrate blocking. Instead, a strong Sc blocking minimum is observed at  $110^\circ$ . The position of this minimum can be assigned according to the stereographic projection of the (111) faced cubic crystal and corresponds to the  $[\bar{1}\bar{1}1]$  blocking direction in the  $[\bar{2}11]$  scattering plane. This provides evidence for a  $60^\circ$  rotation of the  $\text{Sc}_2\text{O}_3$  film relatively to a substrate. To verify this, the sample was rotated azimuthally and aligned in a Si  $[\bar{2}11]$  scattering plane. The Sc angular distribution now shows minima corresponding to a  $[\bar{1}2\bar{1}]$  scattering plane, respectively, which confirms the film rotation.

$\text{Sc}_2\text{O}_3$  and Si have significantly different crystal structures, different bonding, and lattice constants. The bulk lattice constants of Si (5.43 Å) and  $\text{Sc}_2\text{O}_3$  (9.86 Å) are mismatched by 9.2% (relative to the doubled Si unit-cell dimension). It is intriguing that a highly ordered epitaxial growth was obtained with this unusually large mismatch.

The authors wish to thank the Department of Natural Sciences at National Science Council, Taiwan, R.O.C. for supporting this work. The work at Rutgers was supported by the NSF.

<sup>1</sup>J. Kim, R. Mehandru, B. Luo, F. Ren, B. P. Gila, A. H. Onstine, C. R. Abernathy, S. J. Pearton, and Y. Irokawa, *Appl. Phys. Lett.* **81**, 1687 (2002).

<sup>2</sup>C. P. Chen, M. Hong, J. Kwo, H. M. Cheng, Y. L. Huang, S. Y. Lin, J. Chi, H. Y. Lee, Y. F. Hsieh, and J. P. Mannaerts, *Proceedings of the International Conference on Molecular-Beam Epitaxy*, 23–27 August 2004; *J. Cryst. Growth* **278**, 638 (2005).

<sup>3</sup>D. O. Klenov, L. F. Edge, D. G. Schlom, and S. Stemmer, *Appl. Phys. Lett.* **86**, 051901 (2005), and references therein.

<sup>4</sup>A. R. Kortan, M. Hong, J. Kwo, P. Chang, C. P. Chen, J. P. Mannaerts, and S. H. Liou, *Mater. Res. Soc. Symp. Proc.* **811**, E1.2 (2004).

<sup>5</sup>J. F. van der Veen, *Surf. Sci. Rep.* **5**, 199 (1985).

<sup>6</sup>L. G. Parratt, *Phys. Rev.* **95**, 359 (1954).

<sup>7</sup>D. K. Bowen and B. K. Tanner, *Nanotechnology* **4**, 175 (1993).

<sup>8</sup>M. Hong, M. Passlack, J. P. Mannaerts, J. Kwo, S. N. G. Chu, N. Moriya, S. Y. Hou, and V. J. Fratello, *J. Vac. Sci. Technol. B* **14**, 2297 (1996).

<sup>9</sup>M.-W. Chu, I. Szafraniak, R. Scholz, C. Harnagea, D. Hesse, M. Alexe, and U. Gösele, *Nat. Mater.* **3**, 87 (2004).